Temperature-dependent spectral function of a Kondo impurity in an *s*-wave superconductor

Chenrong Liu,[1,2] Yixuan Huang,[1] Yan Chen,[2,*] and C. S. Ting[1,†]
[1]*Texas Center for Superconductivity, University of Houston, Houston, Texas 77204, USA*
[2]*Department of Physics and State Key Laboratory of Surface Physics, Fudan University, Shanghai 200433, China*

(Received 2 January 2019; revised manuscript received 23 April 2019; published 3 May 2019)

Using the numerical renormalization group method, the effect due to a Kondo impurity in an *s*-wave superconductor is examined at finite temperature T. The T behaviors of the spectral function and the magnetic moment at the impurity site are calculated. At $T = 0$, the spin due to the impurity is in a singlet state when the ratio between the Kondo temperature T_k and the superconducting gap $\Delta(0)$ is larger than 0.26. Otherwise, the spin of the impurity is in a doublet state. We show that the separation of the double Yu-Shiba-Rusinov peaks in the spectral function shrinks as T increases if $T_k/\Delta(0) < 0.26$, while it expands if $T_k/\Delta(0) > 0.26$ and $\Delta(0)$ remains constant. These features could be measured by experiments and thus provide a unique way to determine whether the spin of the single Kondo impurity is in the singlet or doublet state at zero temperature.

DOI: 10.1103/PhysRevB.99.174502

I. INTRODUCTION

The quasiparticle states induced by a magnetic impurity with spin $S = 1/2$ in an *s*-wave superconductor (SC) inside the BCS gap are known as the Yu-Shiba-Rusinov (YSR) states [1–5]. At zero temperature T, the spectral function exhibits two δ-function-like peaks symmetrically located at $\pm\varepsilon$ with respect to the center of the superconducting gap. The physics of the YSR states was also extensively studied [6–9] based on theories beyond the mean-field approximation or the perturbation theory. A detailed investigation of the spectral function of the Kondo impurity at $T = 0$ with the Kondo coupling J using the numerical renormalization group (NRG) theory was previously carried out [10]. Recently, the YSR states of a Kondo impurity [11] in an Fe-based SC with spin-orbit coupling were investigated using the Bogoliubov–de Gennes equations in the mean-field level [12]. Moreover, the physics of an Anderson impurity [13] on the interface between a topological insulator and an *s*-wave SC [14] was also analyzed using the NRG method. On the other hand, few experimental and theoretical works exist for the finite-temperature spectral properties inside the SC gap. For an Anderson impurity with an SC lead, Žitko [15] calculated the spectral properties of these subgap states at finite T using the NRG method, and the result shows that the strengths of the YSR peaks become weakened as T rises. For finite-temperature Kondo resonance, Zhang *et al.* [16] detected it on an organic radical weakly coupled to an Au (111) surface by measuring the differential conductance at low temperatures, which can be described by the perturbation theory of the Kondo impurity model. Moreover, Ruby *et al.* [17] probed the single-electron current which passed through the bound states on the superconducting surface and analyzed the relaxation processes of this current to obtain information about the quasiparticle transitions and lifetimes.

Due to the exchange scattering of the thermally excited quasiparticles with the magnetic impurity, there should be nontrivial behaviors in the impurity-site spectral functions at finite T. This problem has never been seriously investigated for a Kondo impurity. It is also essential to understand whether quasiparticles could completely or partially screen the spin of the magnetic impurity in the SC at finite T. In addition, the relationship between the spectral function and the renormalized magnetic moment of the impurity needs to be discussed. In this paper, we investigate the temperature-dependent spectral function and the renormalized magnetic moment at the impurity site using the NRG method. These problems so far have not been studied for the Kondo Hamiltonian. In Appendix A, the energy-evolution calculation of the Kondo impurity system at zero temperature [10] as a function of J (see Fig. 5) is reproduced. If T_k is the Kondo temperature and $\Delta(0)$ is the SC gap at $T = 0$, the spin at the impurity site should be completely screened and is in the singlet state for $T_k/\Delta(0) > 0.26$, while it is in the doublet state for $T_k/\Delta(0) < 0.26$. Our calculation of the magnetic moment due to the impurity at moderate values of T_k indicates that the spin of the single Kondo impurity could be only partially screened by quasiparticles for $T/\Delta(0) > 10^{-2}$. The experimental consequence of our T-dependent spectral function will be addressed.

II. MODEL AND METHOD

We consider the single kondo impurity [11] in an *s*-wave superconductor,

$$\begin{aligned} H &= H_{BCS} + H_{\rm imp}, \\ H_{BCS} &= \sum_{k\sigma} \epsilon_k c^\dagger_{k\sigma} c_{k\sigma} - \Delta(T) \sum_k (c^\dagger_{k\uparrow} c^\dagger_{-k\downarrow} + \text{H.c.}), \\ H_{\rm imp} &= J\boldsymbol{S} \cdot \left(\frac{1}{2N_s} \sum_{kk'\sigma\sigma'} c^\dagger_{k\sigma} \boldsymbol{\tau}_{\sigma\sigma'} c_{k'\sigma'} \right). \end{aligned} \tag{1}$$

*yanchen99@fudan.edu.cn
†ting@uh.edu

Here $c_{k\sigma}$ is the electron annihilation operator at momentum k and spin σ, ϵ_k is the single-particle energy band dispersion, $\Delta(T)$ is the T-dependent BCS gap parameter, J is the antiferromagnetic exchange interaction between the Kondo impurity and the conduction electrons, $\boldsymbol{S}$ is the impurity spin with $S = 1/2$, N_s is the number of lattice sites, and $\boldsymbol{\tau}$ is the Pauli matrix.

Suppose that the bandwidth of the conduction electrons is from $-D$ to D, and the density of states ρ of the conduction electrons is taken to be $\rho = 1/2D$. For the $\Delta(T) = 0$ case, the Kondo temperature in the weak-coupling limit is [10,18–20]

$$T_k = D(J\rho)^{\frac{1}{2}} \exp\left(-\frac{1}{J\rho}\right). \tag{2}$$

This result is based on the Kondo model [11]. The ground state of the spin at the impurity site is completely screened by a conduction electron and becomes a singlet at $T = 0$ regardless of the magnitude of J. The Kondo impurity behaves like a nonmagnetic impurity [21]. It needs to be pointed out that there is another Kondo temperature of T_k^* [22] defined as the half width at half maximum (HWHM) of the Kondo resonance at $T = 0$. To compare our results with those of others, we use both T_k^* and T_k. In Fig. 7 in Appendix B, we compare T_k and T_k^* as functions of J.

In order to carry out the NRG method, one needs to apply the spherical wave representation and to discretize the states of conduction electrons in a logarithmic way. Equation (1) is then transformed into a one-dimensional Wilson chain [10,20]. Its brief description is given at the beginning of Appendix B. One efficient way to optimize the calculation is to set $\Lambda = 2$ and $N_z = 8$ (the interleaved discretization grids, z averaging) [15,18,23–25]. Furthermore, we fixed $\Delta(0)/D = 0.01$ and varied J at $T = 0$. We also employed a finite-temperature SC gap $\Delta(T)$ to perform the calculation of the T-dependent spectral function (see the details in Appendix B). We kept at least 5000 states for the spectrum function calculations.

III. NUMERICAL RESULTS

In Appendix A, we discuss how the energies of the ground and the first excited states of the Hamiltonian (1) are calculated using NRG. The energy evolutions of the doublet and singlet states of the spin at the impurity site are obtained as functions of Kondo coupling J at $T = 0$. This result is shown in Fig. 5. There we rescale the energy value by subtracting the ground state E_0 at $J = 0$. In a weak-coupling region such as $J/D < J_c/D \approx 0.39$, which corresponds to $T_k/\Delta(0) = 0.26$, the impurity spin ($S = 1/2$) could not pair with any conduction electron, and thus, the ground state has doublet degeneracy. For $J > J_c$, it appears that the impurity spin can capture an electron from a Cooper pair and can form a singlet ground state. This result is consistent with the previous calculation of [10]. However, whether this "captured electron" is at the impurity site or not so far has not been investigated. We argue from the feature of the spectral function at the impurity site, and this issue can be answered.

One of the primary efforts here is to obtain the temperature dependence of the spectral function that corresponds to the imaginary part of the T matrix. This type of calculation was performed using the NRG method [10,18,20,26,27]. The method and the definition of the T matrix are described in Appendix B. In Appendix B, we also report the spectral function (see Fig. 6) of a Kondo impurity at $T = 0$ in the presence of a magnetic field h without SC in Fig. 6(a). The spectral function exhibits the Kondo resonance at zero energy for weak h, and the resonant peak will split into two as $g\mu_B h/T_k^* > 0.51$, with $g = 2$ and μ_B being the Bohr magneton. From Fig. 6(b), the transition from a single Kondo resonance to double resonances as h varies appears to be of the first order. These results are consistent with those of Costi [22].

In the presence of SC and a Kondo impurity, it is well known that the double peaks of YSR states in the spectral function at the impurity site are δ-function-like and are located symmetrically with respect to the center of the SC gap. We plot the positions of the YSR peaks as functions of $T_k/\Delta(0)$ at zero T in Fig. 8 (see Appendix B). In the region of $0.9 > T_k/\Delta(0) > 0.26$, the spin due to the impurity is in the singlet state or carries no net magnetic moment. We wish to understand why the in-gap YSR states, which are an essential feature of a magnetic impurity, still exist while the impurity paired with another electron to form the singlet-spin or nonmagnetic state. We argue that when T_k is not too much larger than $\Delta(0)$, the impurity spin may loosely pair with an electron from a Cooper pair to form a singlet. The "paired electron" is not at the impurity site, and locally, the impurity spin still retains its spin-doublet behavior and generates YSR states. However, for $T_k/\Delta(0) > 1$, as shown in the inset of Fig. 8, the two YSR states separately move away from the middle part of the gap and toward the coherent peaks or edges of the gap as $T_k/\Delta(0)$ increases. When $T_k/\Delta(0) = 5.2$ (or $J/D = 0.8$), the YSR peaks at $T = 0$ approach the coherent peaks of the SC gap. For $J/D = 1$, we show that no YSR states exist inside the gap. In this limit, the pairing electron should be tightly bounded to the impurity site, and the spin state at the impurity site becomes a Kondo singlet, which behaves like a nonmagnetic impurity [21].

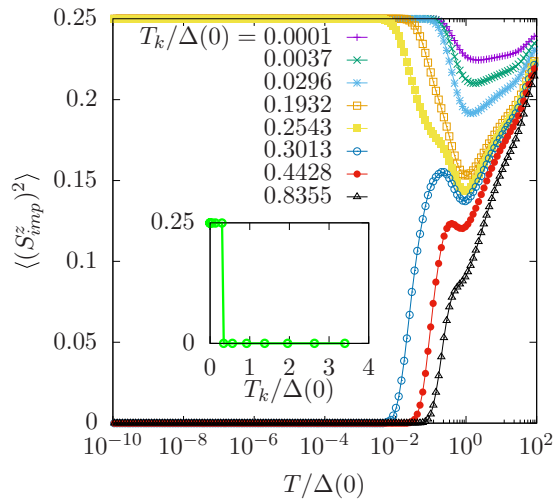

FIG. 1. The square of the impurity magnetization $\langle (S^z_{\rm imp})^2 \rangle$ vs T for different values of $T_k/\Delta(0)$. The inset is the impurity magnetic moment square $\langle (S^z_{\rm imp})^2 \rangle$ at zero temperature. The crossing point is $T_k/\Delta(0) \approx 0.26$ (or $J/D = 0.39$).

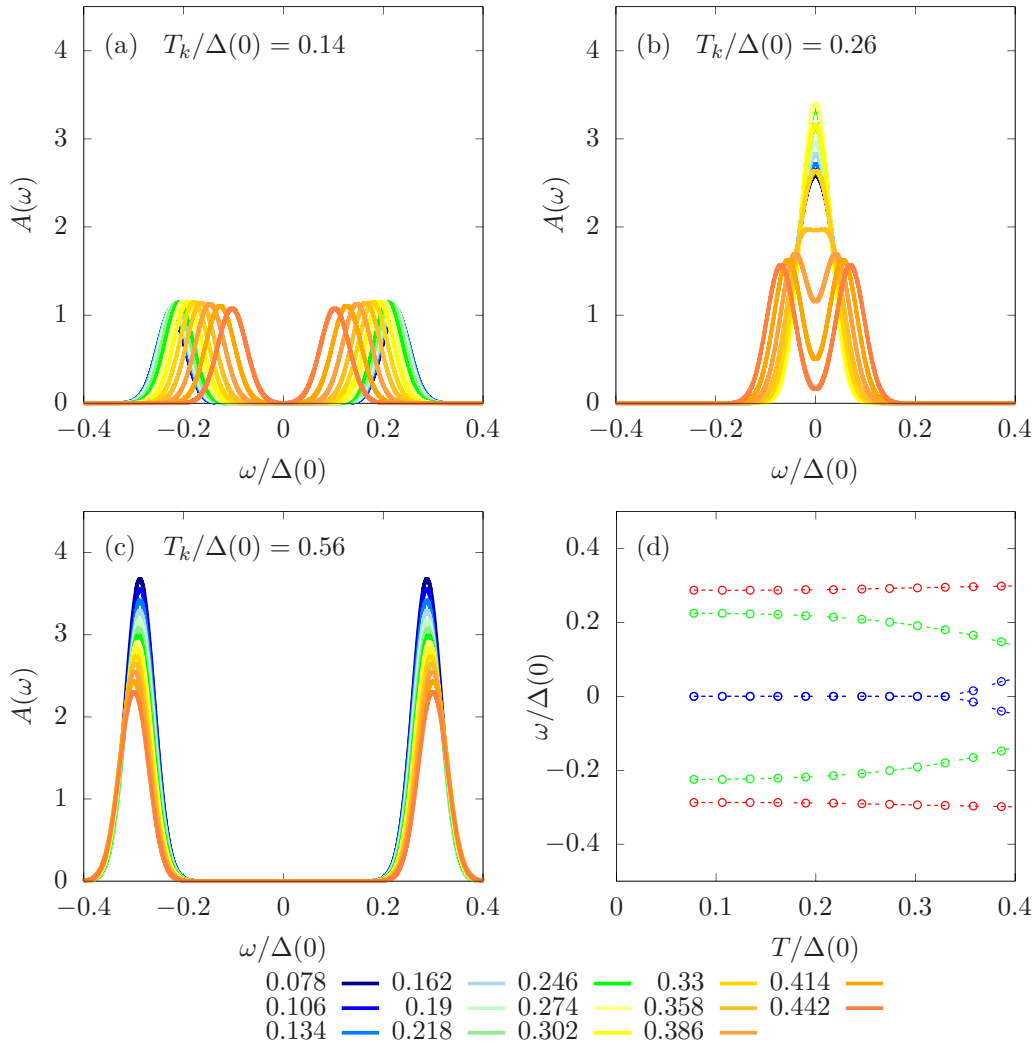

FIG. 2. Spectral functions of the subgap states at finite temperatures. We varied $T/\Delta(0)$ in (a)–(c) while keeping (a) $J/D = 0.35$, $T_k/\Delta(0) = 0.14$, (b) $J/D = 0.39$, $T_k/\Delta(0) = 0.26$, and (c) $J/D = 0.45$, $T_k/\Delta(0) = 0.56$. (d) The YSR peak positions obtained from (a)–(c) vs $T/\Delta(0)$. The green circles correspond to the peak positions in (a) if the T dependence is carried out, blue circles represent the peak positions in (b), and the red circles label the peak positions in (c). The key on the bottom indicates the values of $T/\Delta(0)$.

The square of the impurity magnetic moment $\langle M^2\rangle$ as a function of $T/\Delta(0)$ is calculated for several different values of $T_k/\Delta(0)$ in Fig. 1, where M is the magnetic moment $M = S^z_{\rm imp}$ due to the impurity defined in Appendix C. The curves here show that for $T_k/\Delta(0) < 0.26$ and > 0.26, $\langle M^2\rangle$ equals, respectively, 0.25 (or $S^z_{\rm imp} = 1/2$, a doublet state) and 0 (or $S^z_{\rm imp} = 0$, a singlet state) at $T/\Delta(0) < 10^{-2}$. For $T/\Delta(0) > 10^{-2}$, the impurity spin could be only partially screened by the thermally excited electrons so that $\langle M^2\rangle$ is always less than 0.25. But at $T \gg T_k$, we expect $\langle M^2\rangle$ should approach 0.25, and the spin of the impurity becomes a doublet. The inset showing the variation of $\langle M^2\rangle$ as a function of $T_k/\Delta(0)$ at $T = 0$ is consistent with Figs. 5 and 8 at $T = 0$.

It appears that a doublet to singlet transition exists at $T_k/\Delta(0) \approx 0.26$ for the spin state due to the Kondo impurity at $T = 0$. Let us now examine the spectral functions against $\omega/\Delta(0)$ at the impurity site for three different values of $T_k/\Delta(0)$ and several different temperatures. Here ω measures the bias energy. The results are presented in Figs. 2(a)–2(c). As one can see, as T increases from zero, all the widths of the YSR peaks become broadened. In Fig. 2(a) with $T_k/\Delta(0) = 0.14$ (or $J/D = 0.35$), the impurity spin state is in a doublet at $T = 0$, and the distance between the double YSR peaks shrinks as T increases. In Fig. 2(c) with $T_k/\Delta(0) = 0.56$ (or $J/D = 0.45$), the impurity spin state is a singlet at $T = 0$, and the separation between the double YSR peaks is slightly expanding. One can also look into the spectral function shown in Fig. 2(b) at the critical transition point with $T_k/\Delta(0) \approx 0.26$ (or $J/D = 0.39$). In this case, the double YSR peaks collapse into a single peak at $T = 0$ which could split into two again as $T/\Delta(0) > 0.35$. All these features imply that the critical transition point $T_k/\Delta(0) = 0.26$ at $T = 0$ should move to lower values at finite T. In Fig. 2(d), we plot the positions of YSR peaks shown in Figs. 2(a)–2(c) against $T/\Delta(0)$. The YSR states in the spectral function vs the bias energy ω at the impurity site can easily be measured by scanning tunneling microscopy (STM) experiments. It would be interesting to determine the spin state of the impurity at a very low temperature. This can be accomplished for a Kondo impurity in metal

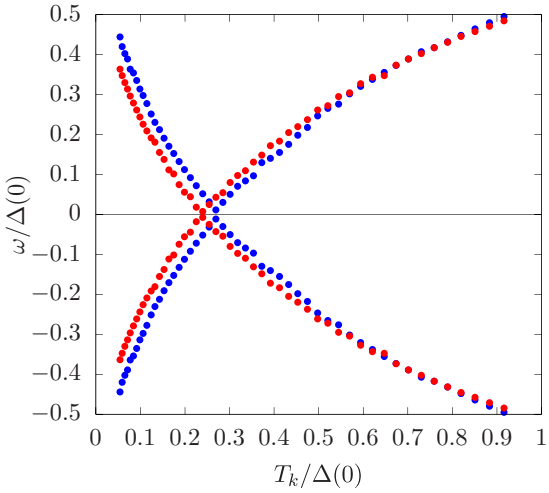

FIG. 3. The subgap YSR peak positions vs $T_k/\Delta(0)$ at $T/\Delta(0)=0$ (blue dots) and $T/\Delta(0) = 0.358$ (red dots).

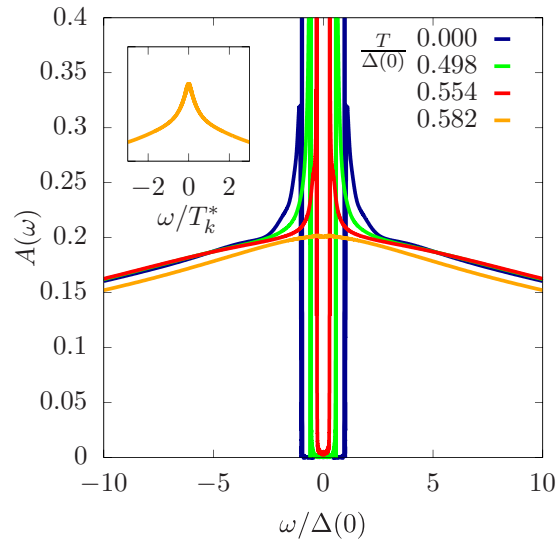

FIG. 4. Spectral functions at $\Delta(T)$, $T_k/\Delta(0) = 5.2$ ($J/D = 0.8$) and several different T. The inset is the curve rescaled by ω/T_k^*.

by measuring its magnetic susceptibility. However, in an SC, the magnetic susceptibility of the impurity cannot be detected; then the finite-T behaviors exhibited in Fig. 2 can provide an unambiguous way to determine the spin state due to the magnetic impurity. For instance, if the distance between the YSR peaks is shrinking as T increases, the spin state at $T = 0$ is a doublet, and if it is slightly increasing, then the impurity spin state should be a singlet. The above conclusion is valid only when the SC gap $\Delta(T)$ decreases slightly as T is raised from very low T to a higher temperature $T < 2/3T_c$, which should be true for the SC gap in BCS theory; here T_c is the SC transition temperature. As T approaches T_c, the separation between the YSR peaks will always be decreasing with $\Delta(T)$ regardless of the value of $T_k/\Delta(0)$.

The T-dependent behavior of the YSR peak positions is shown to originate from the T-dependent SC gap $\Delta(T)$. The broadening of the YSR peaks is due to the thermally excited quasiparticles. But if one fixes $\Delta(T) = \Delta(0)$ as a T-independent quantity, then the peak positions will not be changed with T, as previous work has demonstrated for an Anderson impurity [15]. We are also able to obtain the same behavior for a Kondo impurity by setting $\Delta(T) = \Delta(0)$. In the present work, however, we set $\Delta(T)$ as the BCS SC gap at finite T, which has the expression shown in Eq. (B13) in Appendix B.

To better understand what has been done in Fig. 2, we plot the positions of YSR peaks from the spectrum function vs $T_k/\Delta(0)$ in Fig. 3. The curve with blue dots obtained at $T = 0$ is identical to that in Fig. 8, and the curve with red dots is calculated for $T/\Delta(0) = 0.358$. This result clearly indicates that the critical point $T_k/\Delta(0) \approx 0.26$ at zero temperature is moving to the weaker Kondo coupling region at finite T.

So far we have studied the spectrum function only for moderate strength of $T_k/\Delta(0)$ (< 0.9). For an impurity with strong Kondo coupling such as that shown in the inset of Fig. 8 with $T_k/\Delta(0) > 5.0$, the YSR peaks move toward the edges or merge with coherent peaks of the SC gap. In Fig. 4, we present the spectral function at the impurity site with $T_k/\Delta(0) = 5.2$ or $J/D = 0.8$ for several different values of T. It can be seen that the YSR peaks are very close to the coherent peaks at $T/\Delta(0) = 0$. At finite T, the two YSR peaks become broadened and merge completely with the coherent peaks at not too low temperatures. It appears that there are no longer YSR states inside the SC gap. For $T/\Delta(0) = 0.582 > T_c/\Delta(0) = 0.57$, the SC no longer exists in the system, and a broad peak (the orange curve) centered at $\omega = 0$ shows up. We replot the orange curve using a different energy scale, $\omega/\ T_k^*$, in the inset, which exhibits the Kondo resonance at finite temperature without the SC. We also numerically calculated the integrated weight of the YSR peaks as a function of J/D at $T = 0$; the result is shown in Fig. 9 in Appendix B. It is demonstrated there that as J/D approaches 0 and 1, the integrated weight of the YSR peaks goes to 0. The maximum integrated weight comes around $J/D = 0.5$. For $J = 0$, there is no Kondo impurity, and there are no YSR peaks. For $J/D = 1$, the YSR peaks are at the coherent peaks but with zero integrated weight, and those are the typical characteristics of a nonmagnetic impurity in which the impurity spin paired strongly with the spin of a conduction electron at the impurity site to form a rigid singlet state. The behavior for J/D close to 1 is also consistent with the result for an Anderson impurity [28].

IV. CONCLUSION

We have studied the evolutions of the ground state and first excited energies of the Kondo Hamiltonian with a SC at $T = 0$ as functions of $T_k/\Delta(0)$. There the ground state is a doublet for $T_k/\Delta(0) < 0.26$ and a singlet for $T_k/\Delta(0) > 0.26$. On the other hand, the spin at the impurity site is always in the doublet state unless it can pair with an electron at the impurity site to form a singlet state in the region of

$T_k/\Delta(0) > 5.0$. Determining whether the sample under experimental measurements is in the doublet or singlet spin state at $T = 0$ is an important issue to address. We also showed that the separation between the double YSR peaks in the spectral function decreases as T is raised for $T_k/\Delta(0) < 0.26$, while it increases slightly as T is raised to $T < 2/3T_c$ for $T_k/\Delta(0) > 0.26$. This feature should be measurable by STM experiments, and the result could be used to unambiguously determine the spin state of the system at $T = 0$. The T-dependent spectral function for a strong Kondo impurity with $T_k/\Delta(0) = 5.2$ or $J/D = 0.8$ was also calculated, and we found that the YSR peaks are very close to the edges of the SC gap at $T = 0$. For $J/D = 1$, we demonstrated that the YSR peaks are at the coherent peaks of the SC but with zero weight, which is characteristic of a nonmagnetic impurity with a singlet spin state [21].

ACKNOWLEDGMENTS

We are thankful for the help from Dr. R. Žitko and the useful discussions with Dr. J.-X. Zhu. Work at Houston is supported by the Robert A. Welch Foundation under Grant No. E-1146 and the Texas Center for Superconductivity at the University of Houston. Work at Fudan University is supported by the National Key Research and Development Program of China (Grants No. 2017YFA0304204 and No. 2016YFA0300504), the National Natural Science Foundation of China (Grants No. 11625416 and No. 11474064), and the Shanghai Municipal Government under Grant No. 19XD1400700.

APPENDIX A: ENERGY EVOLUTION WITH KONDO COUPLING AT ZERO TEMPERATURE

Using the NRG iteration diagonalization, it is easy to obtain the ground-state energy and the first excitation energy. Here the number of sites on the Wilson chain is about 68, and that is enough for high precision of diagonalization. After the last NRG iteration step, we can pick up the energy values. This is the energy level of the system. Thus, we can get the lowest energies. We notice here that the lowest energies may locate in a different Hilbert space which is labeled by a good quantum number.

We first calculate the lowest two energy-level evolutions of the system by varying the Kondo coupling J at $T = 0$. Near $J = 0$, the state of the impurity is a spin doublet in the ground state; the first excited state corresponds to the excitation from a Cooper pair at the impurity site, and one of the quasiparticles is then captured by the impurity spin to form a singlet state as long as J is finite. This result is shown in Fig. 5. Here we rescale the energy value by subtracting the ground state E_0 at $J = 0$. In the weak-coupling case as $J/D < J_c/D \approx 0.39$, corresponding to $T_k/\Delta(0) = 0.26$, the impurity spin ($S = 1/2$) could not pair with any conduction electron, and thus, the ground state has doublet degeneracy. For $J > J_c$, it appears that the impurity spin can capture an electron from a Cooper pair and can form a singlet ground state. This result was also obtained by previous calculations in [10] and indicates that the impurity spin cannot be partially screened.

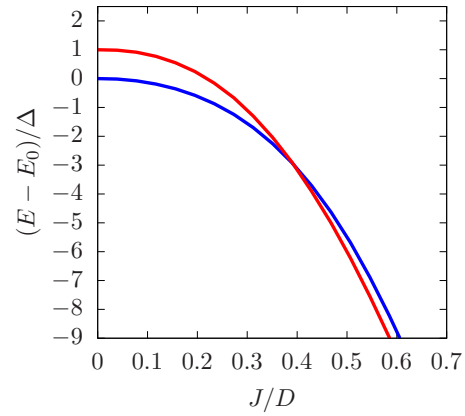

FIG. 5. The evolutions of the impurity spin-doublet-state energy (blue curve) and the impurity spin-singlet-state energy (red curve) as a function of J with $\Delta(0)/D = 0.01$ and $T = 0$.

APPENDIX B: THE WILSON CHAIN AND THE SPECTRUM FUNCTION

According to Refs. [10,20], after applying the spherical wave representation, Eq. (1) transforms into the Wilson chain,

$$\begin{aligned} H &= H_k + H_\Delta + H_{\rm imp}, \\ H_k &= \frac{1+\Lambda^{-1}}{2}\sum_\sigma\sum_{n=0}^{\infty}\Lambda^{-n/2}\epsilon_n(f^\dagger_{n\sigma}f_{n+1\sigma} + \text{H.c.}), \\ H_\Delta &= -\Delta\sum_{n=0}^{\infty}(f^\dagger_{n\uparrow}f^\dagger_{n\downarrow} + \text{H.c.}), \\ H_{\rm imp} &= \frac{J}{2}\boldsymbol{S}\cdot\sum_{\sigma\sigma'}f^\dagger_{0\sigma}\boldsymbol{\tau}_{\sigma\sigma'}f_{0\sigma'}, \end{aligned} \tag{B1}$$

and

$$\begin{aligned} \epsilon_n = (1-\Lambda^{-(n+1)})(1-\Lambda^{-(2n+1)})^{-1/2} \\ \times(1-\Lambda^{-(2n+3)})^{-1/2}, \end{aligned} \tag{B2}$$

where Λ ($\Lambda > 1$) is a logarithmic discretization parameter and we normalized the density of states of conduction electrons by $D = 1$. From Eq. (B1), the first site is the impurity site, while the other sites are electron sites. The Wilson chain is a half-infinity chain, which means it starts from the impurity and ends at the infinity site. However, it is impossible to add infinity number sites. Because the coefficient of the hopping term in Eq. (B1) shows power-law decay with the number of sites, it can be cut off at site N_s. N_s is 68 in our calculations, and it depends on the convergence accuracy. We also kept 5000 states at each iteration of the diagonalization. After that, the Hamiltonian can be solved numerically.

The T matrix is defined as [29]

$$\begin{aligned} T_\sigma &= -i\theta(t)\langle[O_\sigma(t), O_\sigma(0)^\dagger]_+\rangle, \\ O_\sigma &= [H_{\rm imp}, f_{0,\sigma}]_+, \end{aligned} \tag{B3}$$

which describes the scattering of conduction electrons off the impurity. Since we know $H_{\rm imp}$, the operator O_σ can be written

as

$$O_\sigma = JS \cdot \sum_{\sigma'} \frac{1}{2} \boldsymbol{\tau}_{\sigma\sigma'} f_{0,\sigma'}. \tag{B4}$$

The spin spectral function is

$$A_\sigma(\omega) = -\frac{1}{\pi} \mathrm{Im} \tilde{T}_\sigma(\omega + i\delta). \tag{B5}$$

We obtain the impurity spectral function by summing the up- and down-spin spectral function [22],

$$A(\omega) = \sum_\sigma A_\sigma(\omega), \tag{B6}$$

where $\tilde{T}$ is the Fourier transformation of T in ω space. Then, we apply the full-density-matrix (FDM) NRG method [30] in the actual finite-temperature spectral function calculations. After that, we accumulate the raw spectral data and use 1000 bins as well as two different broadening kernels, one inside the gap and another one outside [31]. To calculate the finite-temperature spectral function, we use the FDM method for high accuracy [30,32]. It takes advantage of a complete set of the discarded numerical renormalization group eigenstates. Assuming $|s\rangle_n^X$ is the eigenstate of the Wilson chain Hamiltonian at the iteration diagonalization step n, X indicates K (kept states) or D (discarded states), and the length of the total chain is N. Then, we can build the approximate eigenstates of the total Hamiltonian [30],

$$H_N |se\rangle_n^X \approx E_s^n |se\rangle_n^X, \tag{B7}$$

where $|se\rangle_n^X = |s\rangle_n^X \otimes |e_n\rangle$, $|e_n\rangle = |\sigma_N\rangle \otimes \cdots \otimes |\sigma_{n+1}\rangle$ are the so-called environmental states, and $|\sigma_n\rangle$ are the single-site states $|0\rangle$, $|\uparrow\rangle$, $|\downarrow\rangle$, and $|\uparrow\downarrow\rangle$. The E_s^n state has d^{N-n}-fold degeneracy. These discarded states from all the iteration diagonalization steps can be combined into a complete eigenstate $|se\rangle_n^D$ of H_N,

$$\sum_{n>n_0}^{N} \sum_{se} |se\rangle_{n\,n}^{DD} \langle se| = 1, \tag{B8}$$

where n_0 is the last step that can be calculated without truncation in the iteration diagonalization. These states are called the Anders-Schiller basis [33,34]. The full density matrix is

$$\rho \approx \sum_{n>n_0} \sum_{se} |se\rangle_n^D \frac{e^{-\beta E_s^n}}{Z} {}_n^D \langle se| = \sum_{n>n_0} \omega_n \rho_{DD}^n, \tag{B9}$$

where $\rho_{DD}^n = |se\rangle_{n\,n}^{DD} \langle se|$ is the density matrix for the *discarded* states at the nth $(n > n_0)$ step of the Wilson chain iteration diagonalization and $\omega_n = d^{N-n} Z_n^D / Z$, where $Z_n^D = \sum_s^D e^{-\beta E_s^n}$, $Z = \sum_{se} e^{-\beta E_s^n}$. Therefore, we always have the following relations:

$$\mathrm{Tr}\left[\rho_{DD}^n\right] = 1, \tag{B10}$$

$$\sum_{n>n_0} \omega_n = 1. \tag{B11}$$

The thermal averaged spectral function becomes

$$A(\omega) = \sum_{n>n_0} \omega_n A_n(\omega). \tag{B12}$$

$A_n(\omega)$ is the spectral function calculated in the Anders-Schiller basis at the nth step of the iteration diagonalization process.

To calculate the finite-T spectral function, we use two different broadening kernels, as we mentioned in the main text. A modified log-Gaussian broadening kernel was used in the gap region, and the broadening parameter α is 0.0004. A Gaussian broadening kernel was used outside the region, and the broadening parameter $\omega_0 = T$. We do this broadening and the spectral function calculations by writing a PERL script to call the NRG LJUBLJANA library.

Because the BCS gap parameter Δ is temperature dependent, we also use $\Delta(T)$ instead of the constant number Δ in the calculations of the temperature-dependent spectrum functions. In fact, it is hard to consider a self-consistent process in the NRG to determine the BCS parameter $\Delta(T)$ in the Hamiltonian. Therefore, we keep $\Delta(0)/D = 0.01$ at $T = 0$ and use a phenomenological expression BCS gap formula to simulate the real situation [15],

$$\Delta(T) \approx \delta_{SC} T_c \tanh\left[\frac{\pi}{\delta_{SC}} \sqrt{a \frac{\delta C}{C_N} \left(\frac{T_c}{T} - 1\right)}\right], \tag{B13}$$

where $\delta_{SC} = 1.76$, $a = 2/3$, $\delta C/C_N = 1.43$. This is a good approximation for the true case with $T \to 0$ and $T \to T_c$.

To test our numerical method, let us study the Kondo problem at $T = 0$ without the SC [or $\Delta(0) = 0$] in the presence of an applied magnetic field h. The spectral function exhibits the well-known Kondo resonant behavior at zero energy for a weak magnetic field [see Fig. 6(a)], and the resonance peak will split into two as h becomes more significant than a critical value h_c, which can be obtained from $g\mu_B h_c / T_k^* \approx 0.51$, where $g = 2$ is the g factor and μ_B is the Bohr magneton.

These results are consistent with those of Costi's calculation [22]. In addition, we also calculate the peak positions as a function of the magnetic field h, and the transition appears to be first order, as shown in Fig. 6(b). Here the Kondo temperature T_k^* [22] is defined as the HWHM of the Kondo resonance at $T = 0$. A comparison of T_k^* and the traditional Kondo temperature T_k as functions of J is shown in Fig. 7. It is easy to see that their difference grows larger as J increases.

Furthermore, we plot the positions of the YSR peaks as functions of $T_k/\Delta(0)$ in Fig. 8. The double YSR peaks emerge from the SC coherent peaks in the gap region as T_k or J changes from zero to a finite value (not shown here). As $T_k/\Delta(0)$ increases, the separation between the YSR peaks shrinks, and it vanishes at $T_k/\Delta(0) \approx 0.26$. Figure 5 in Appendix A indicates that for $T_k/\Delta(0) < 0.26$ or $J/D < 0.39$, the spin state at the impurity site is a doublet, which implies that the impurity spin is not even partially screened. When $T_k/\Delta(0) > 0.26$, the double YSR peaks show up again in the gap, the spin state becomes a singlet, and the magnetic impurity changes to nonmagnetic. A similar result was also obtained by another group [10].

The spectral function in NRG is computed by broadening the raw δ peak binned into narrow intervals and is hence a continuous function that can easily be integrated numerically. As we mentioned in the main text, we numerically calculated the integrated weight of the YSR peaks as a function of J/D

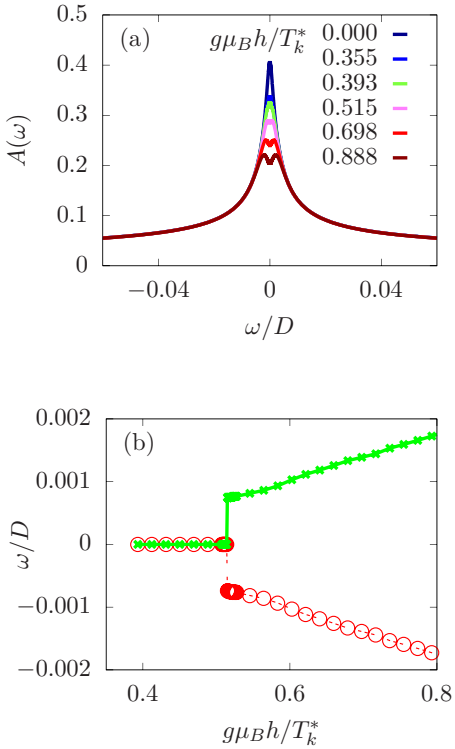

FIG. 6. Spectral functions with the magnetic field at $\Delta(T) = 0$, $T = 0$. (a) Kondo resonance and its splitting in the presence of a magnetic field h and (b) the positions of the splitting peaks as a function of h.

at $T = 0$. The integrated weight of the YSR peak is defined as $W_{YSR} = \int_a^b A(\omega)d\omega$ [15], where a and b are points to the left and the right of the YSR peak. It is demonstrated in Fig. 9 that as J/D approaches 0 and 1, the integrated weight of the YSR peaks goes to 0. The maximum integrated weight comes around $J/D = 0.5$. For $J = 0$, there is no Kondo impurity, and there are no YSR peaks. For $J/D = 1$, the YSR peaks are at the coherent peaks but with zero integrated weight (Fig. 9), and that is a typical characteristic of a nonmagnetic impurity in which the impurity spin pairs strongly with the spin of a

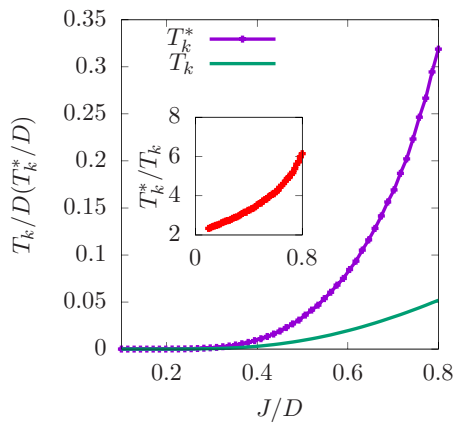

FIG. 7. Comparison between T_k and T_k^* as functions of J/D. The inset shows the ratio T_k^*/T_k as a function of J/D.

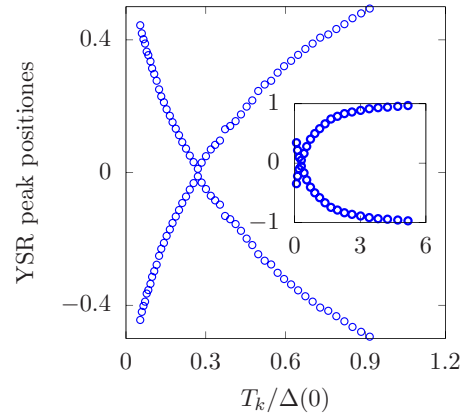

FIG. 8. Zero-temperature YSR peak positions. The positions of the YSR peaks in the spectral function plotted against $T_k/\Delta(0)$ at $T = 0$. The crossing point is $J_c/D \approx 0.39$ [or $T_k/\Delta(0) = 0.26$].

conduction electron at the impurity site to form a rigid singlet state.

APPENDIX C: THE SQUARE OF THE IMPURITY MAGNETIC MOMENT

Although the particle number is not conserved in the original Hamiltonian, the system still has spin $U(1)$ symmetry. Thus, the Wilson chain can be diagonalized in the S_z subspace. After completing the diagonalization process, it is easy to obtain the two lowest energy levels by comparing all the lowest-energy values in all of the subspace.

Since the total S_z is a good quantum number, the square of the impurity magnetic moment is expressed as [18,35,36]

$$\left\langle \left(S_{\text{imp}}^z\right)^2 \right\rangle = \left\langle \left(s_{\text{imp}}^z + S^z\right)^2 \right\rangle - \langle (S^z)^2 \rangle_0, \tag{C1}$$

where $S^z = \sum_{i=1}^{Ns} s_i^z$ and s_i^z is the spin of the Wilson chain at site i. Here s_{imp}^z is the spin at the impurity site, and $\langle \cdots \rangle$ indicates the value is measured in the system with a Kondo impurity, while $\langle \cdots \rangle_0$ represents this measurement for the clean system. Such a quantity reflects the changes in magnetic moment due to the presence of the impurity. If there are no

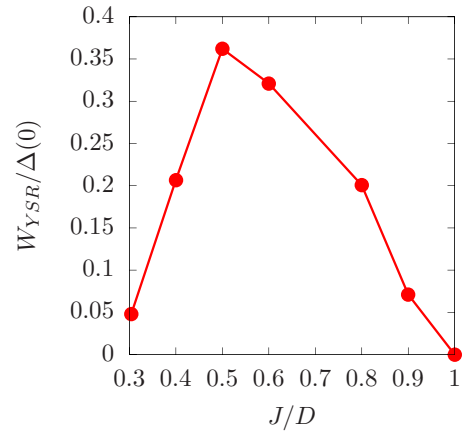

FIG. 9. Integrated weight of the YSR peak at $T = 0$. The weight goes to zero when the YSR peak moves closer to the coherent peak.

conduction electrons, $\langle (S^z_{\rm imp})^2 \rangle$ is just 0.25. Similarly, it is zero if no impurity exists. Thus, Eq. (C1) describes the impurity contribution to the square of the magnetic moment. Also, we using the z averaging and finite-temperature NRG algorithm to perform the T-dependent thermal property calculations.

Two competing interactions exist in the system; one is the Kondo coupling, and the other is SC pairing. In the weak Kondo coupling case, all the conduction electrons form Cooper pairs, and the impurity is not able to capture an electron from the Cooper pair. In this case, $\langle (S^z_{\rm imp})^2 \rangle$ is 0.25, or its square root measuring $\langle S^z_{\rm imp} \rangle$ is 0.5. On the other hand, once the Kondo coupling J becomes stronger but not too strong that $T_k/\Delta(0) > 0.26$, the impurity can pair loosely with an electron from a Cooper pair to form a singlet state. However, this electron can go to sites away from the impurity and still form a Cooper pair with another electron. Therefore, the impurity may still maintain some of its magnetic behavior. For $J \gg J_c$, the impurity can capture an electron, and it may behave like a nonmagnetic impurity, as we mentioned in the main text. Moreover, $\langle (S^z_{\rm imp})^2 \rangle$ is zero if $T_k/\Delta(0) > 0.26$.

[1] Y. Lu, Acta Phys. Sin. **21**, 75 (1965).
[2] H. Shiba, Prog. Theor. Phys. **40**, 435 (1968).
[3] A. Rusinov, J. Exp. Theor. Phys. **29**, 1101 (1969).
[4] A. V. Balatsky, I. Vekhter, and J.-X. Zhu, Rev. Mod. Phys. **78**, 373 (2006).
[5] A. Yazdani, B. A. Jones, C. P. Lutz, M. F. Crommie, and D. M. Eigler, Science **275**, 1767 (1997).
[6] E. Müller-Hartmann and J. Zittartz, Phys. Rev. Lett. **26**, 428 (1971).
[7] K. Y. Guslienko, V. Novosad, Y. Otani, H. Shima, and K. Fukamichi, Phys. Rev. B **65**, 024414 (2001).
[8] M. Matsumoto and M. Koga, J. Phys. Soc. Jpn. **70**, 2860 (2001).
[9] K. C. Lukas, W. S. Liu, G. Joshi, M. Zebarjadi, M. S. Dresselhaus, Z. F. Ren, G. Chen, and C. P. Opeil, Phys. Rev. B **85**, 205410 (2012).
[10] O. Sakai, Y. Shimizu, H. Shiba, and K. Satori, J. Phys. Soc. Jpn. **62**, 3181 (1993).
[11] J. Kondo, Prog. Theor. Phys. **32**, 37 (1964).
[12] Y.-Y. Tai, H. Choi, T. Ahmed, C. S. Ting, and J.-X. Zhu, Phys. Rev. B **92**, 174514 (2015).
[13] P. W. Anderson, Phys. Rev. **124**, 41 (1961).
[14] R. Wang, W. Su, J.-X. Zhu, C. S. Ting, H. Li, C. Chen, B. Wang, and X. Wang, Phys. Rev. Lett. **122**, 087001 (2019).
[15] R. Žitko, Phys. Rev. B **93**, 195125 (2016).
[16] Y.-h. Zhang, S. Kahle, T. Herden, C. Stroh, M. Mayor, U. Schlickum, M. Ternes, P. Wahl, and K. Kern, Nat. Commun. **4**, 2110 (2013).
[17] M. Ruby, F. Pientka, Y. Peng, F. von Oppen, B. W. Heinrich, and K. J. Franke, Phys. Rev. Lett. **115**, 087001 (2015).
[18] K. G. Wilson, Rev. Mod. Phys. **47**, 773 (1975).
[19] N. Andrei, K. Furuya, and J. H. Lowenstein, Rev. Mod. Phys. **55**, 331 (1983).
[20] K. Satori, H. Shiba, O. Sakai, and Y. Shimizu, J. Phys. Soc. Jpn. **61**, 3239 (1992).
[21] H. Suhl and D. Wong, Phys. Physics (Long Island City, NY) **3**, 17 (1967).
[22] T. A. Costi, Phys. Rev. Lett. **85**, 1504 (2000).
[23] H. O. Frota and L. N. Oliveira, Phys. Rev. B **33**, 7871 (1986).
[24] W. C. Oliveira and L. N. Oliveira, Phys. Rev. B **49**, 11986 (1994).
[25] R. Žitko and T. Pruschke, Phys. Rev. B **79**, 085106 (2009).
[26] R. Bulla, T. A. Costi, and T. Pruschke, Rev. Mod. Phys. **80**, 395 (2008).
[27] R. Žitko, NRG LJUBLJANA, 2017, http://nrgljubljana.ijs.si.
[28] J. Bauer, A. Oguri, and A. C. Hewson, J. Phys.: Condens. Matter **19**, 486211 (2007).
[29] L. Fritz, S. Florens, and M. Vojta, Phys. Rev. B **74**, 144410 (2006).
[30] A. Weichselbaum and J. von Delft, Phys. Rev. Lett. **99**, 076402 (2007).
[31] T. Hecht, A. Weichselbaum, J. von Delft, and R. Bulla, J. Phys.: Condens. Matter **20**, 275213 (2008).
[32] L. Merker, A. Weichselbaum, and T. A. Costi, Phys. Rev. B **86**, 075153 (2012).
[33] F. B. Anders and A. Schiller, Phys. Rev. Lett. **95**, 196801 (2005).
[34] F. B. Anders and A. Schiller, Phys. Rev. B **74**, 245113 (2006).
[35] H. R. Krishna-murthy, J. W. Wilkins, and K. G. Wilson, Phys. Rev. B **21**, 1044 (1980).
[36] P. S. Cornaglia and C. A. Balseiro, Phys. Rev. B **66**, 115303 (2002).